Electrohydrodynamic instabilities and orientation of dielectric ellipsoids in low-conducting fluids

A. Cēbers
Institute of Physics, University of Latvia, Salaspils-1, LV-2169, Latvia

E. Lemaire and L. Lobry
Laboratoire de Physique de la Matière Condensée (CNRS UMR No. 6622), Parc Valrose, 06108 Nice Cedex 2, France
(Received 5 June 2000; published 18 December 2000)

We study the dynamics of an ellipsoidal particle in a weakly conducting dielectric liquid when submitted to a dc electric field. At low field intensities, the particle long axis is aligned in the field direction. When the field strength is increased, we show that, depending on the initial orientation of the particle, there exist two stable orientations: the one with the long axis parallel to the field direction remains possible while a spinning state with the long axis perpendicular to the field appears. This last striking orientation is due to the finite Maxwell-Wagner polarization relaxation time. For sufficiently high field intensities, each state loses its stability and the particle dynamics becomes chaotic. Those conclusions from the theoretical model are supported by experimental observations.

DOI: 10.1103/PhysRevE.63.016301 PACS number(s): 47.52.+j, 77.84.Nh, 77.22.Ej

I. INTRODUCTION

A broad class of physical phenomena is connected with various electrohydrodynamic instabilities in liquid crystals [1,2]. Equally interesting and complex is the behavior of dielectric suspensions under the action of an electric field where various electrohydrodynamic phenomena can occur. For instance, we can mention the formation of the zig-zag band structure arising in a suspension of charged colloidal particles under a strong alternating electric field [3,4] or the formation of similar structures in DNA solutions [5]. The mechanism responsible for the formation of this pattern has been linked with the perturbation of the ionic distribution taking place far beyond the double layer around the aggregate of polyions in the electrolyte [6]. This deviation from the electroneutrality coupled with the action of a field can lead to electroconvection and colloidal separation.

Another class of electrohydrodynamic phenomena exists where the corresponding mechanism responsible for the instability is connected with the finite polarization relaxation time. The noninstantaneous relaxation of the polarization has been used to explain, for example, the recirculation of ferromagnetic particles in an ellipsoidal drop of ferrofluid arising in an alternating magnetic field [7]. Another more popular example of this kind of phenomenon is the electrohydrodynamic instability leading to the so-called Quincke rotation, discovered at the end of the 19th century [8]: a dielectric body surrounded by a low conducting liquid spontaneously rotates when submitted to a sufficiently high dc electric field. The necessary and sufficient condition for the body to rotate is that the charge relaxation time $\tau=\epsilon/\sigma$ in the solid is larger than in the surrounding liquid ($\tau_2>\tau_1$) [9,10]. Some interesting consequences on the behavior of a dielectric suspension follow from the Quincke rotation. Indeed, the spinning of dielectric particles can cause ''negative'' viscosity effects to appear in a dielectric suspension [11,12]. Recently it was proved experimentally [13] that the spontaneous rotation of dielectric particles due to the convective charge transfer increases drastically the effective conductivity of a suspension [14].

In this paper we present another manifestation of the finite polarization relaxation time effect: the complex behavior of an insulating elongated ellipsoidal particle surrounded by a low conducting liquid and submitted to a dc field. We show that this behavior is governed by a competition between the instantaneous component of the polarization coming from the permittivity difference between the particle and the liquid and its retarding part originating in the free charges accumulation on the particle surface. This study has started in [11] where it has been established that the single stable steady orientation direction of the long axis of the particle that could exist at an electrical field strength below a critical value was along the direction of the external field. It has been shown that the critical electric field value at which this orientation lost its stability increased with the axis ratio of the particle. The complex dynamics of an ellipsoidal dielectric particle due to the finite interfacial polarization time has been investigated at a later stage in [15,16], where regimes of a chaotic dynamics and a limit cycle have been identified.

Herein we demonstrate that, when the spontaneous rotation of the particle around its long axis is taken into account, a stable orientation perpendicular to the external dc field appears. For a definite range of electrical field strengths, the two stable orientations—parallel and transversal to the external field—can coexist. In this sense our results extend the results obtained by Jones [17], who has shown that different equilibrium orientations of an ellipsoid exist only under the action of an ac field.

The paper is organized as follows. In the next section, we introduce the theoretical model. The dynamics of the ellipsoid is fully determined by the relaxation equations of the polarization and by the balance of angular momentum. In Sec. III, we present the different stationary orientations of the particle and, using a perturbation method, we discuss their stability. Section IV contains several qualitative and

quantitative experimental results confirming the main conclusions from the theoretical model. Finally the conclusions are drawn in Sec. V.

II. THEORETICAL MODEL

The total interfacial polarization can be split up into two parts: the instantaneous polarization $\boldsymbol{P}^{\infty}$ coming from the permittivity mismatch and the retarding polarization $\boldsymbol{P}$ that originates in the free charges accumulation. The polarization of an ellipsoidal particle is defined by the three components P_i $(i=1\ldots3)$ and the three components P_i^{∞} $(i=1\ldots3)$ in the reference frame that moves and rotates with the particle. In the following, we consider an axisymmetric body whose symmetry axis is along x_3. P_1 and P_2 are the components of the retarding polarization perpendicular to the symmetry axis. The equations of electrostatic and the charge conservation lead to the following relaxation equations for P_i [15,16]:

$$\frac{\partial P_1}{\partial t}=-\frac{1}{\tau_{\perp}}[P_1-(\chi_{\perp}^0-\chi_{\perp}^{\infty})E_1], \tag{1a}$$

$$\frac{\partial P_2}{\partial t}=-\frac{1}{\tau_{\perp}}[P_2-(\chi_{\perp}^0-\chi_{\perp}^{\infty})E_2], \tag{1b}$$

$$\frac{\partial P_3}{\partial t}=-\frac{1}{\tau_{\parallel}}[P_3-(\chi_{\parallel}^0-\chi_{\parallel}^{\infty})E_3], \tag{1c}$$

where $\tau_{\parallel,\perp}$ are the characteristic times for the polarization to relax along the symmetry axis and perpendicularly to it,

$$\tau_{\parallel,\perp}=\frac{\epsilon_0((\epsilon_2-\epsilon_1)n_{\parallel,\perp}+\epsilon_1)}{(\sigma_2-\sigma_1)n_{\parallel,\perp}+\sigma_1}. \tag{2}$$

The high-frequency susceptibilities $\chi_{\parallel,\perp}^{\infty}$ depend on the permittivities of the fluid and of the particle

$$\chi_{\parallel,\perp}^{\infty}=\frac{\epsilon_0\epsilon_1 V(\epsilon_2-\epsilon_1)}{(\epsilon_2-\epsilon_1)n_{\parallel,\perp}+\epsilon_1}, \tag{3}$$

whereas the static susceptibilities $\chi_{\parallel,\perp}^{0}$ are determined by the conductivity values

$$\chi_{\parallel,\perp}^{0}=\frac{\epsilon_0\epsilon_1 V(\sigma_2-\sigma_1)}{(\sigma_2-\sigma_1)n_{\parallel,\perp}+\sigma_1}, \tag{4}$$

where $n_{\parallel,\perp}$ are the depolarization factors.

The electrophysical properties with subscript ''2'' characterize the material of the particle, whereas those with index ''1'' refer to the surrounding fluid.

The inertia of the particle and that of the fluid are neglected, the balance of the viscous and electrical torque in the set of coordinates connected with the particle leads to

$$-\alpha_{\perp}\Omega_1+[\boldsymbol{P}^{\infty}\times\boldsymbol{E}]_1+[\boldsymbol{P}\times\boldsymbol{E}]_1=0, \tag{5a}$$

$$-\alpha_{\perp}\Omega_2+[\boldsymbol{P}^{\infty}\times\boldsymbol{E}]_2+[\boldsymbol{P}\times\boldsymbol{E}]_2=0, \tag{5b}$$

$$-\alpha_{\parallel}\Omega_3+[\boldsymbol{P}\times\boldsymbol{E}]_3=0, \tag{5c}$$

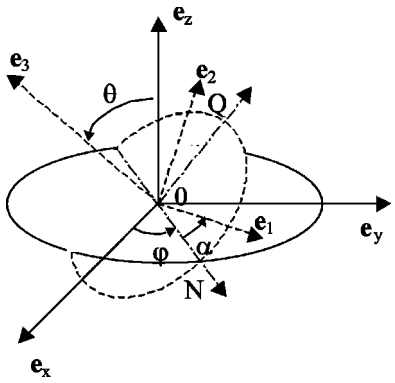

FIG. 1. Definition of the reference frame.

where $\alpha_{\parallel,\perp}$ are the rotational friction coefficients.

The components of the instantaneous polarization of the particle $\boldsymbol{P}^{\infty}$ due to the permittivity mismatch between the particle and the fluid are defined by

$$P_{1,2}^{\infty}=\chi_{\perp}^{\infty}E_{1,2}, \tag{6}$$

$$P_3^{\infty}=\chi_{\parallel}^{\infty}E_3. \tag{7}$$

Introducing the Euler angles θ,ϕ,α as usual (Fig. 1), expressing the components of the angular velocity $\boldsymbol{\Omega}$ according to the relations [18]

$$\Omega_1=\dot{\phi}\sin\theta\sin\alpha+\dot{\theta}\cos\alpha, \tag{8a}$$

$$\Omega_2=\dot{\phi}\sin\theta\cos\alpha-\dot{\theta}\sin\alpha, \tag{8b}$$

$$\Omega_3=\dot{\phi}\cos\theta+\dot{\alpha}, \tag{8c}$$

and introducing the polarization components P_N in the nodal line direction and P_Q in the $(\boldsymbol{e}_3\times\boldsymbol{0N})$ direction,

$$P_N=P_1\cos\alpha-P_2\sin\alpha, \tag{9}$$

$$P_Q=P_2\cos\alpha+P_1\sin\alpha, \tag{10}$$

the set of equations (1) and (5) can be transformed into

$$\dot{\theta}=\frac{1}{\alpha_{\perp}}[-(\chi_{\parallel}^{\infty}-\chi_{\perp}^{\infty})E_3E_Q+E_3P_Q-P_3E_Q], \tag{11a}$$

$$\dot{\phi}=-\frac{1}{\alpha_{\perp}}\frac{P_NE_3}{\sin\theta}, \tag{11b}$$

$$\dot{\alpha}=\frac{P_NE}{\sin\theta}\left(\frac{\sin^2\theta}{\alpha_{\parallel}}+\frac{\cos^2\theta}{\alpha_{\perp}}\right), \tag{11c}$$

and equations for the electric polarization could be rewritten as

$$\frac{\partial P_N}{\partial t}+\dot{\alpha}P_Q=-\frac{1}{\tau_{\perp}}P_N, \tag{12a}$$

$$\frac{\partial P_Q}{\partial t} - \dot{\alpha} P_N = -\frac{1}{\tau_\perp}[P_Q - (\chi_\perp^0 - \chi_\perp^\infty)E_Q], \tag{12b}$$

$$\frac{\partial P_3}{\partial t} = -\frac{1}{\tau_\parallel}[P_3 - (\chi_\parallel^0 - \chi_\parallel^\infty)E_3], \tag{12c}$$

where $E_3 = E\cos\theta$, $E_Q = E\sin\theta$, and $E_N = 0$ since the polar axis has been chosen along the direction of the external electric field. Let us make several remarks before undertaking the analysis of the equilibrium states of the particle and their stability. First, it follows from Eqs. (11) and (12) that a closed set of equations can be obtained for θ, P_N, P_Q, and P_3. Second, the convective terms on the left side of the first two equations (12) can be written as $-[\dot{\alpha}\boldsymbol{e}_3 \times \boldsymbol{P}]_{\parallel,\perp}$ and are related to the convective transport of the interfacial charges upon the rotation of a particle around its revolution axis.

III. STATIONARY STATES AND THEIR STABILITY

Looking for stationary solutions of the set of equations for the variables θ, P_N, $P_\perp$, and P_3 we obtain the following set of equations:

$$E_3 E_Q = 0, \tag{13}$$

$$P_N = -\tau_\perp \dot{\alpha} P_Q, \tag{14}$$

$$P_Q(1 + (\tau_\perp \dot{\alpha})^2) = (\chi_\perp^0 - \chi_\perp^\infty)E_Q, \tag{15}$$

$$P_3 = (\chi_\parallel^0 - \chi_\parallel^\infty)E_3. \tag{16}$$

If $E_Q = 0$, then $\theta = 0$ and $P_N = P_Q = 0$, $P_3 = (\chi_\parallel^0 - \chi_\parallel^\infty)E$. From the last equation of the set (11) it follows that $\dot{\alpha} = 0$. This solution corresponds to an orientation with the long axis of the particle along the direction of the external field.

Another solution corresponds to $E_3 = 0$. That means that $\theta = \pi/2$ and $P_3^0 = 0$,

$$P_Q^0 = \frac{(\chi_\perp^0 - \chi_\perp^\infty)E}{1 + (\tau_\perp \dot{\alpha})^2}, \tag{17}$$

$$P_N^0 = -\frac{\tau_\perp \dot{\alpha}(\chi_\perp^0 - \chi_\perp^\infty)E}{1 + (\tau_\perp \dot{\alpha})^2}. \tag{18}$$

This second stationary solution corresponds to a state of the particle rotating around itself along its revolution axis oriented perpendicularly to the direction of the electric field. In the following, we will term it the transversal state. In this case the last equation of the set (11) gives

$$(\dot{\alpha}\tau_\perp)^2 = -\frac{(\chi_\perp^0 - \chi_\perp^\infty)\tau_\perp E^2}{\alpha_\parallel} - 1. \tag{19}$$

This solution with nonzero $\dot{\alpha}$ exists if the electric field satisfies the following condition:

$$E^2 > E_{c\perp}^2 = -\frac{\alpha_\parallel}{\tau_\perp(\chi_\perp^0 - \chi_\perp^\infty)}. \tag{20}$$

We should mention that for this last condition to be possible, it is necessary that $\chi_\perp^0 < \chi_\perp^\infty$.

Let us now consider the stability of these two stationary solutions. The stability of the spinless state has been considered in [15,16] where it has been shown that it lost its stability through a Hopf bifurcation when an electric field higher than $E_{\parallel\star\star}$ was applied:

$$E_{\parallel\star\star} = \sqrt{-\frac{\alpha_\perp}{\tau_\perp(\chi_\parallel^0 - \chi_\perp^\infty)}}. \tag{21}$$

To determine the stability of the transversal state, we study the evolution of the deviation angle $\theta' = \theta - \pi/2$ from the equilibrium. For small deviation, the relations (11a) and (12c) give

$$\alpha_\perp \dot{\theta}' = (\chi_\parallel^\infty - \chi_\perp^\infty)E^2\theta' - EP_Q^0\theta' - P_3'E, \tag{22}$$

$$\frac{\partial P_3'}{\partial t} = -\frac{1}{\tau_\parallel}[P_3' + (\chi_\parallel^0 - \chi_\parallel^\infty)E\theta']. \tag{23}$$

Equations (22) and (23) for the growth increment λ of the small perturbation $\theta', P_3' \approx \exp(\lambda t)$ give

$$\lambda = \frac{-a \pm \sqrt{a^2 - 4b}}{2\alpha_\perp \tau_\parallel}, \tag{24}$$

where

$$a = \alpha_\perp + \tau_\parallel(\chi_\perp^0 - \chi_\perp^\infty)E_{c\perp}^2 + \tau_\parallel(\chi_\perp^\infty - \chi_\parallel^\infty)E^2, \tag{25a}$$

$$b = \alpha_\perp \tau_\parallel((\chi_\perp^0 - \chi_\perp^\infty)E_{c\perp}^2 + (\chi_\perp^\infty - \chi_\parallel^0)E^2). \tag{25b}$$

We see that four cases exist: (i) $a > 0$, $b < 0$, unstable; (ii) $a < 0$, $b < 0$, unstable; (iii) $a < 0$, $b > 0$, unstable; (iv) $a > 0$, $b > 0$, stable. Thus, for the spinning state to be stable it is necessary to satisfy the two following conditions:

$$(\chi_\perp^0 - \chi_\perp^\infty)E_{c\perp}^2 + (\chi_\perp^\infty - \chi_\parallel^0)E^2 > 0 \tag{26}$$

and

$$\alpha_\perp + \tau_\parallel(\chi_\perp^0 - \chi_\perp^\infty)E_{c\perp}^2 + \tau_\parallel(\chi_\perp^\infty - \chi_\parallel^\infty)E^2 > 0. \tag{27}$$

Since, for the existence of the spinning state, the condition $\chi_\perp^0 < \chi_\perp^\infty$ is necessary, then condition (26) can be fulfilled only if $\chi_\perp^\infty - \chi_\parallel^0 > 0$. Thus, we obtain the threshold electrical field above which the spinning state is stable,

$$E^2 > \frac{(\chi_\perp^\infty - \chi_\perp^0)E_{c\perp}^2}{(\chi_\perp^\infty - \chi_\parallel^0)} = E_{\perp\star}^2. \tag{28}$$

Since $\chi_\perp^\infty - \chi_\perp^0 > \chi_\perp^\infty - \chi_\parallel^0$ the spinning state can become stable only for an electric-field value larger than the critical electric field $E_{c\perp}$ above which the particle is able to rotate around

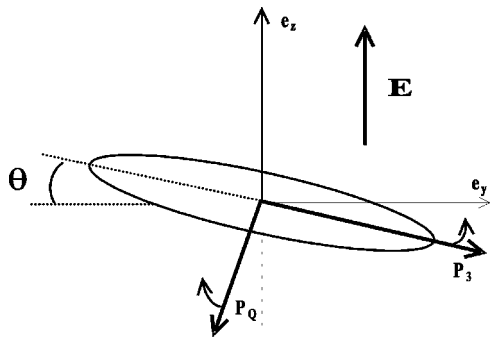

FIG. 2. Schematic explanation of the stabilization of the transversal orientation by the rotation. P_3 exerts a restoring torque on the particle, while the torque exerted by the component P_Q tends to increase the deviation. As the angular velocity of the particle increases, the polarization component P_Q diminishes.

itself along its long axis direction. The physical reason why the rotation along the long axis may cause the stabilization of the transversal orientational state is quite simple. Let us consider a slight deviation of the particle from its transversal orientation. Since the component P_3 of the polarization is in the direction opposite to the electric field, it exerts a restoring torque on the particle, while the torque exerted by the component P_Q tends to increase the deviation (see Fig. 2). As the angular velocity of the particle increases, the polarization component P_Q diminishes, then the restoring torque arising from P_3 becomes sufficient to put back the particle in its equilibrium position. It should be noted that the necessity of a sufficient diminution of P_Q to observe the transversal state is consistent with the inequality $E_{\perp\star} > E_{c\perp}$.

For still higher applied fields the spinning transversal state loses its stability. Indeed, seeing that $\chi_{\parallel}^{\infty} - \chi_{\perp}^{\infty} > 0$, the second condition (27) imposes a superior limit $E_{\perp\star\star}$ on the electric field for the transversal state to remain stable:

$$E_{\perp\star\star}^2 = \frac{(\chi_{\perp}^{\infty} - \chi_{\perp}^{0})}{(\chi_{\parallel}^{\infty} - \chi_{\perp}^{\infty})} E_{c\perp}^2 \left(\frac{\tau_{\perp} \alpha_{\perp}}{\tau_{\parallel} \alpha_{\parallel}} - 1 \right). \tag{29}$$

Since at the critical field strength $E_{\perp\star\star}$, $a=0$ and $b>0$, it follows from the expression (24) that a supercritical Hopf bifurcation takes place and a limit cycle behavior arises.

Let us compare the value $E_{\perp\star}$ with electric-field strength $E_{\parallel\star\star}$ at which the parallel orientation of the particle becomes unstable. From relations (21) and (28), we can write

$$E_{\perp\star}^2 = \frac{\alpha_{\parallel}}{\alpha_{\perp}} E_{\parallel\star\star}^2. \tag{30}$$

Since for an elongated particle $\alpha_{\parallel} < \alpha_{\perp}$, the spinning state becomes stable before the parallel orientation loses its stability. This means that there exists a range of electric fields in which both states are stable—the parallel spinless state and the transversal spinning state. The physical parameters determine which state loses its stability first. Figure 3 is an illustration of the coexistence of the two orientations. We have represented the dependence of $E_{c\perp}^2$ (line 2) and $E_{\perp\star}^2$ (line 1) on the axis ratio a/b calculated with the physical parameters

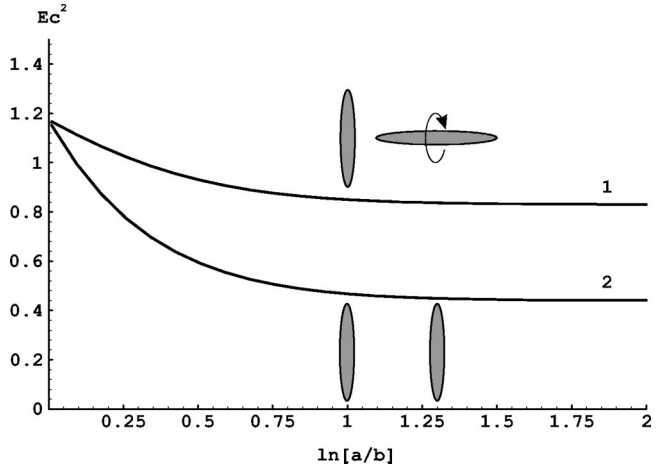

FIG. 3. Critical electric fields squared are normalized by $2\eta\sigma_1/(\epsilon_0\epsilon_1)^2$ versus $\ln(a/b)$. Line 2 represents $E_{c\perp}$, the field above which the particle is able to rotate around itself along its long axis in the transversal state. Line 1 represents $E_{\perp\star}$, the field above which this state is stable.

corresponding to the experiments described in the next section ($\sigma_2 = 0, \epsilon_2 = 5, \epsilon_1 = 4.4$). The critical electric fields squared are normalized by $2\eta\sigma_1/(\epsilon_0\epsilon_1)^2$ and the axis ratio is plotted in semilogarithmic coordinates. For electric fields higher than $E_{\perp\star}$ two possible stationary states exist—spinless with the particle symmetry axis along the field and spinning transversal state. The model predicts that it is the parallel orientation that first disappears. Due to the high value compared to $E_{\perp\star}$, $E_{\parallel\star\star}$ is not plotted on the graph.

IV. EXPERIMENTAL OBSERVATIONS

We have observed the orientation of elongated polyamide fibers (length $2a = 1$ mm and diameter $2b = 25$ μm) suspended in a mixture of transformer oil and another dielectric liquid (Ugilec, Elf Atochem). The mixture is made in order

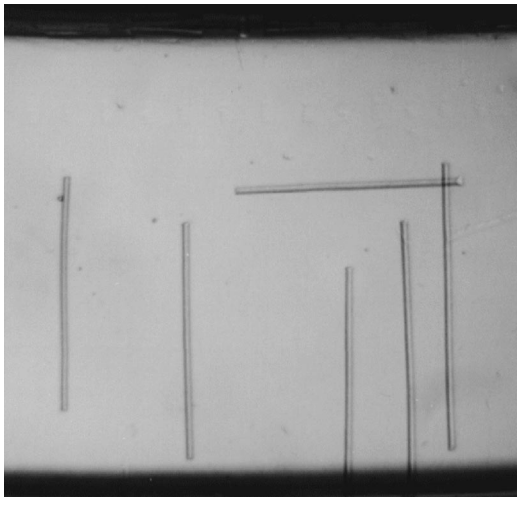

FIG. 4. Experimental observation of the coexistence of the both orientations—spinless parallel state and spinning transversal state—above $E_{\perp\star}$.

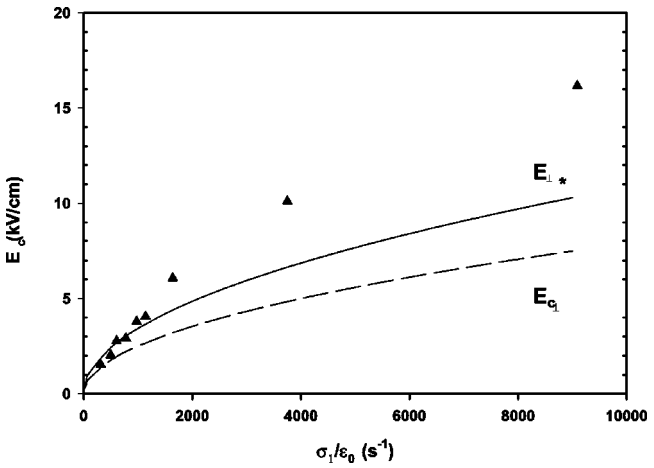

FIG. 5. Comparison of the predictions (solid line) and the experimental measurements (symbols) of $E_{\perp\star}$ versus σ_1/ϵ_0. The dashed line represents the variation of $E_{c\star}$.

to match the density of fibers ($\rho=1.15$ g/cm^3). The viscosity of the liquid is 12 cP. Its dielectric permittivity has been measured using an impedance analyzer (4192A LF, Hewlett Packard) and has been found to be equal to 4.4. The conductivity of the liquid is controlled by adding AOT salts [bis(2-ethylhexyl)sulfosuccinate sodium]. In any case, the conductivity of the fibers is much lower (100 to 1000 times) than that of the liquid; their dielectric permittivity is 5. The dc electric field is applied between two stainless-steel electrodes separated one from the other by 2 mm. Experimental observations confirm the predictions of the model: (i) for low applied field values, fibers orient their long axis along the field direction; (ii) above a critical field two stable orientations coexist, depending on the orientation of the fibers before the application of the electric field. Some fibers are aligned along the field direction, while others are perpendicular to it and exhibit spinning behavior.

Figure 4 represents some fibers submitted to a field larger than $E_{\perp\star}$: the coexistence of both parallel and transversal orientations is visible. Furthermore, we observed that each time the fiber is perpendicular to the field, it is rotating around itself.

In Fig. 5 we have plotted the variation of $E_{\perp\star}$ with the conductivity of the liquid. These values are obtained by applying a field higher than $E_{\perp\star}$ and then by decreasing the field intensity until the transversal orientation disappears. The dashed line represents the predictions of the model for the values of $E_{c\perp}$, and the solid line is the prediction for the field $E_{\perp\star}$. The qualitative agreement between experimental results and predictions of our model is fairly good. In particular, we measure a square root dependence of $E_{\perp\star}$ on the conductivity of the fluid. The quantitative discrepancy can have different origins. The first one is the hydrodynamic interactions between fibers and the walls of the cell. Indeed, since all the dimensions are comparable (fiber length 1 mm, gap between the electrodes 2 mm, height of the cell 4 mm), the effective rotational friction coefficients are higher than bulk coefficients. Another explanation could be connected with the electrical interactions between the fibers and their electrostatic images, which may increase the stability of the transversal state.

We have not been able to measure the critical fields for the loss of the stability of both the orientations. Indeed, due to the large axis ratio of the fibers we have used ($\alpha_\perp/\alpha_\parallel \simeq 200$), the critical electric fields $E_{\parallel\star\star}$ and $E_{\perp\star\star}$ are higher by more than one order of magnitude than $E_{\perp\star}$, and electrical breakdowns occur before we reach these critical fields.

V. CONCLUSIONS

According to the theoretical model that takes into account the rotation of an anisotropic particle around its long and short axes, there exists a range of electric field where two stable orientations coexist: a spinless state with the long axis parallel to the electric field and a spinning transversal state. This conclusion from the theoretical model is supported by the experimental observations. We have not be able to observe the stability losses of these states. Nevertheless, we have performed numerical simulations to study the dynamics of the fiber above the critical fields $E_{\perp\star\star}$ and $E_{\parallel\star\star}$. For our experimental parameters, the loss of stability of the spinless state occurs through a supercritical Hopf bifurcation. Otherwise, we have shown previously [15,16] that for another set of values (for instance $\chi_\parallel^0/\chi_\perp^0=\frac{3}{2}$ and $\chi_\parallel^\infty/\chi_\perp^\infty=3$) the Hopf bifurcation was subcritical and that chaotic dynamics took place. For these last parameters, numerical simulations show that the loss of the stability of the transversal state at $E_{\perp\star\star}$ occurs through a supercritical Hopf bifurcation. The fiber oscillates around its equilibrium orientation with a precession around the field direction.

[1] P. De Gennes, *Physics of Liquid Crystals* (Clarendon Press, Oxford, 1974).
[2] M. J. Stephen and J. P. Straley, Rev. Mod. Phys. **46**, 617 (1974).
[3] B. R. Jennings and M. Stankiewicz, Proc. R. Soc. London, Ser. A **427**, 321 (1990).
[4] H. Isambert, A. Ajdari, J. L. Viovy, and J. Prost, Phys. Rev. Lett. **78**, 971 (1997).
[5] L. Mitnik, C. Heller, J. Prost, and J. L. Viovy, Science **267**, 219 (1995).
[6] H. Isambert, A. Ajdari, J. L. Viovy, and J. Prost, Phys. Rev. A **56**, 5688 (1997).
[7] A. Cebers and G. Bossis, Magn. Gidrodin. **34**, 311 (1998).
[8] G. Quinke, Ann. Phys. Chem. **59**, 417 (1896).
[9] J. R. Melcher, IEEE Trans. Educ. **E-17**, 100 (1974).
[10] T. B. Jones, IEEE Trans. IAS **IA-20**, 845 (1984).
[11] A. Cebers, Magn. Gidrodin. **N2**, 81 (1980) (in Russian).
[12] E. Lemaire and L. Lobry, J. Electrost. **47**, 61 (1999).
[13] A. Cebers, E. Lemaire, and L. Lobry, in *2nd International Workshop on Electrical Conduction, Convection and*

Breakdown in Fluids, Grenoble, France, 2000, edited by P. Atten and A. Denat (unpublished).
[14] A. Cebers, Appl. Math. Mech. (USSR) **39**, 1093 (1977) (in Russian).
[15] A. Cebers, Magn. Gidrodin. **N3**, 17 (1991).
[16] A. Cebers, J. Magn. Magn. Mater. **122**, 277 (1993).
[17] T. B. Jones, *Electromechanics of Particles* (Cambridge University Press, Cambridge, England, 1995).
[18] L. D. Landau and E. M. Lifshitz, *Mechanics* (Nauka, Moscow, 1965).